THE GREAT 1964 PRINCE WILLIAM SOUND, ALASKA, EARTHQUAKE: ESTIMATION OF STRONG GROUND MOTION

G. P. Mavroeidis[1], B. Zhang[2], G. Dong[3], A. S. Papageorgiou[4], U. Dutta[5], and N. N. Biswas[6]

[1] *Assistant Professor, Department of Civil Engineering, The Catholic University of America, Washington, DC 20064, USA*
[2] *Senior Researcher, Wilson Center for Research and Technology, Xerox Corporation, Webster, NY 14580, USA*
[3] *Senior Specialist, Technip USA Inc., Houston, TX 77079, USA*
[4] *Professor, Department of Civil Engineering, University of Patras, Patras 26500, Greece*
[5] *Associate Professor, School of Engineering, University of Alaska Anchorage, Anchorage, AK 99508, USA*
[6] *Professor Emeritus, Geophysical Institute, University of Alaska Fairbanks, Fairbanks, AK 99775, USA*

Email: mavroeidis@cua.edu

ABSTRACT

We are generating physically plausible near-field synthetic ground motions for the Great 1964 Prince William Sound, Alaska, earthquake compatible with available seismological data, tectonic information and eyewitness accounts. The objectives of this study are summarized as follows: (a) Simulation of the low-frequency ($f <$ 0.03Hz) strong ground motions on selected locations and on a dense grid of observation points extending over the shallow dipping causative fault of the 1964 Alaska earthquake. In order to accomplish this task, we are utilizing the slip model proposed by Johnson et al. (1996) based on a joint inversion of tsunami waveforms and geodetic data. The calculations are carried out using the discrete wavenumber representation method and the generalized transmission and reflection coefficient technique; (b) Reconstruction of the strong ground motion time histories and response spectra that the city of Anchorage experienced during the 1964 Alaska earthquake. The low-frequency ($f <$ 0.03Hz) ground motions are generated using the methodology described previously. The intermediate-frequency (0.03Hz $< f <$ 0.50Hz) ground motions are simulated by convolving Green's functions generated by the discrete wavenumber representation method with far-field radiation pulses of circular cracks. The high-frequency (0.5Hz $< f <$ 8.0Hz) ground motions are simulated using the stochastic modeling approach. The three independently derived ground motion components are then properly combined to generate synthetic broadband ground motion time histories and response spectra for the city of Anchorage due to the 1964 Prince William Sound earthquake; and (c) Validation of the synthetic strong ground motions for the 1964 Alaska earthquake against observed tectonic deformation, ground motion estimates inferred by descriptions of structural damage, and eyewitness accounts. In summary, the present study provides synthetic time histories and response spectra for engineering applications compatible with all available information pertaining to the 1964 Prince William Sound earthquake. It should be noted however that the generated strong ground motions are not necessarily unique, nor reflect the entire uncertainty that characterizes the problem under investigation.

KEYWORDS: 1964 Alaska earthquake, ground motion simulation, deterministic modeling, stochastic modeling, synthetic time histories, synthetic response spectra, subduction zone

1. INTRODUCTION

The March 28, 1964 Prince William Sound, Alaska, earthquake is one of the greatest seismic events that have occurred in historic times and the second largest instrumentally recorded earthquake with moment magnitude M_w 9.2. It occurred along the eastern part of the Aleutian megathrust in south-central Alaska where the oceanic Pacific plate is being subducted beneath the continental North American plate in a north-northwest direction at about 6cm/yr. Figure 1 illustrates a location map of south-central Alaska along with the epicenter of the 1964 Prince William Sound main shock as determined by Sherburne et al. (1969) and the boundary of the aftershock sequence.

The extensive infrastructure damage in continental Alaska and the generation of large tsunami due to the 1964 Prince William Sound earthquake had a significant impact on the United States National Seismic Hazard Mitigation Program. No strong motion instruments were operational / installed in the vicinity of the 1964

Alaska earthquake when the destructive seismic event occurred. Therefore, no direct measurement of the intensity, duration or frequency content of the actual near-field strong ground motion is available in the form of time histories or response spectra. Only estimates of characteristic ground motion parameters (e.g., peak ground acceleration, peak spectral acceleration, duration of seismic excitation) exist based on information inferred from observed structural damage and eyewitness accounts.

The primary objective of this study is to generate physically plausible near-field synthetic ground motions for the 1964 Prince William Sound earthquake compatible with available seismological data, tectonic information, and eyewitness accounts. We are generating low-frequency strong ground motions on selected location and on a dense grid of points extending over the shallow dipping fault of the 1964 Alaska earthquake, as well as synthetic broadband ground motion time histories and response spectra for the city of Anchorage. The simulated ground motions are then validated against available information (i.e., seismological, tectonic, eyewitness accounts). The generated strong ground motions are not necessarily unique, nor incorporate the total uncertainty that characterizes the problem under investigation. It should be noted that detailed results pertaining to this study are presented by Mavroeidis et al. (2008).

2. SYNTHESIS OF LONG-PERIOD STRONG GROUND MOTION

2.1. Simulation Approach

Fault Slip Model: For the simulation of the low-frequency ($f < 0.03$Hz) strong ground motions due to the 1964 Prince William Sound earthquake, we are using the slip model proposed by Johnson et al. (1996) based on a joint inversion of tsunami waveforms and geodetic data. The slip model consists of eighteen subfaults whose projection onto the free surface is displayed in Figure 2. Half of the subfaults exhibit pure dip-slip mechanisms, while the remaining subfaults have a secondary left-lateral strike-slip component in addition to the primary dip-slip mechanism. The amount of slip on the subfaults varies significantly from 0 to 22.1m with an average value of 8.6m.

Slip Function: A ramp slip function is considered to describe the variation of slip on a specific point on the fault plane as a function of time. We assume that the slip velocity of the 1964 Alaska earthquake was ~100cm/s, a typical value frequently considered by seismologists (e.g., Brune, 1970; Aki, 1983). Consequently, the rise time can be estimated by dividing the amount of slip on each subfault by the characteristic slip velocity. This procedure yields a maximum rise time of approximately 25s for subfaults in the epicentral area.

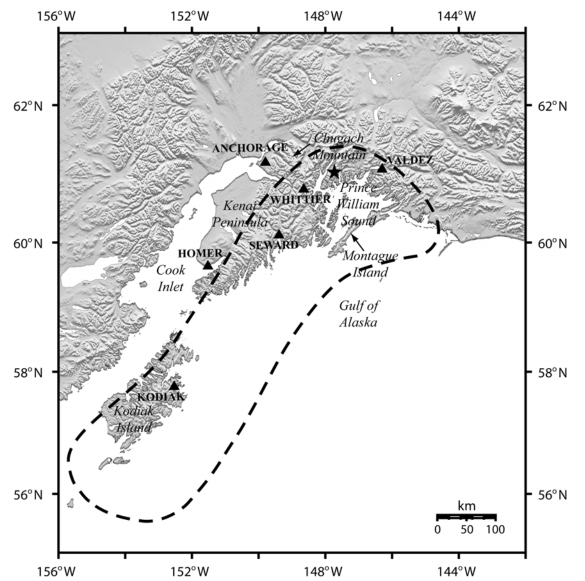

Figure 1. Location map of the Great 1964 Prince William Sound, Alaska, earthquake.

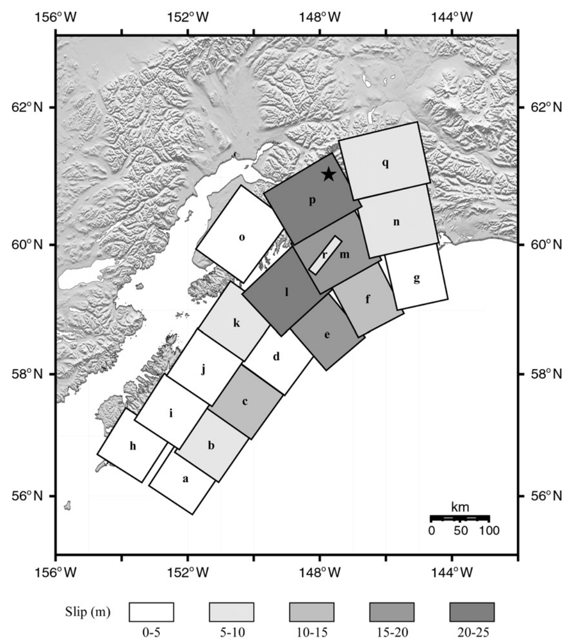

Figure 2. Slip distribution of the 1964 Alaska earthquake based on a joint inversion of tsunami waveforms and geodetic data (Johnson et al., 1996).

Rupture Propagation and Velocity: Several researchers have estimated the rupture velocity towards an average rupture direction (or azimuth) based on seismological data of the 1964 Alaska earthquake (e.g., Furumoto, 1965; Wyss and Brune, 1967; Kanamori, 1970; Christensen and Beck, 1994). There is a consensus among them that the rupture velocity was approximately 3.0 to 3.5km/s towards S20^{o}W to S30^{o}W. In this study, we are adopting the values proposed by Kanamori (1970) for the magnitude and average direction of the rupture velocity; that is, 3.5km/s towards S25^{o}W. We further assume that the rupture front propagated elliptically on the fault plane with: (a) the major axis of the ellipse coinciding with the average rupture direction (S25^{o}W), (b) the first focus of the ellipse coinciding with the epicenter of the 1964 Alaska earthquake, (c) the rupture front along the major axis moving with a velocity equal to the fault rupture velocity, and (d) the eccentricity of the ellipse selected to adequately fit the six distinct subevents defined by Wyss and Brune (1967) in terms of the corresponding time lags. With reference to the abovementioned rupture propagation scheme, we define the rupture initiation at each subfault as the time instant that the elliptical rupture front first reaches/intersects a subfault corner point.

Crustal Model and Computational Method: A one-dimensional simplified crustal model appropriate for south-central Alaska is utilized in our simulations. The simplified model consists of three flat layers lying over a half-space. The computation of the low-frequency seismic motion due to the propagating rupture front of the 1964 Alaska earthquake is carried out using the discrete wavenumber representation method (Bouchon and Aki, 1977; Bouchon, 1979). The generalized transmission and reflection coefficient technique (Luco and Apsel, 1983) is exploited for the propagation of the wavefield through the layered half-space. Long-period synthetic ground motions are produced at selected locations coinciding with major cities and towns in the vicinity of the 1964 Alaska earthquake and at the node points of a dense quadrangular network covering a large part of south-central Alaska.

2.2. Simulation Results

The spatial variation of the generated NS, EW and vertical ground displacement components over a time window of 330s is displayed in Figure 3. The directions pointing north, east and downwards define the positive sign convention of the synthetic ground motion time series. Our forward simulation results yield significant displacement offsets over the extended area that coincides with the projection of the 1964 fault system. These displacement offsets however decay rapidly for regions located away from the fault. Very large amounts of permanent tectonic deformation are predicted for sites lying over the Prince William Sound and Kodiak Island asperities. In the Prince William Sound region, the NS component is the prominent one with a maximum static displacement of ~23m towards south at an offshore site E-SE of Kenai Peninsula. In the same region, the EW and vertical displacement components are also characterized by large offsets (~5m towards east and ~4m uplift, respectively), though an order of magnitude smaller than the displacement offsets computed in the NS direction. On the other hand, in the Kodiak Island region, the NS and EW displacement components are characterized by permanent offsets of comparable size; their peak values are ~7m and ~9m towards south and east, respectively, at a location just east of Kodiak Island. In the same region, the peak vertical displacement offset is less than 2m.

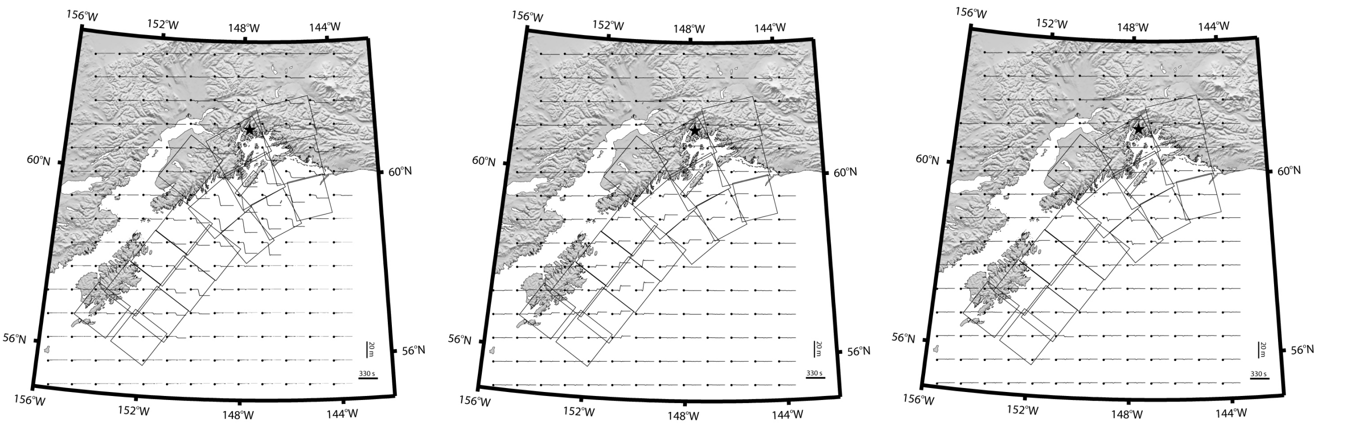

Figure 3. Spatial variation of the low-frequency ground displacement components (NS, EW, vertical from left to right) over a time window of 330s.

3. SYNTHESIS OF BROADBAND STRONG GROUND MOTION AT ANCHORAGE

3.1. Simulation Approach

We are simulating broadband strong motion time histories at Anchorage due to the 1964 Prince William Sound earthquake. The low-frequency (f < 0.03Hz) ground motions are generated using the methodology described in the previous section. The intermediate-frequency (0.03Hz < f < 0.50Hz) ground motions are simulated by convolving Green's functions generated by the discrete wavenumber representation method (Bouchon and Aki, 1977; Bouchon, 1979) with far-field radiation pulses of symmetrical (Sato and Hirasawa, 1973) or asymmetrical (Dong and Papageorgiou, 2002) circular cracks. Several scenarios are examined with variations in the stress drop, radius, number and location of cracks (see Figure 4). The examined scenarios do not cover all possible configurations; they consider however a wide range of realistic radius (15 to 38 km) and stress drop (100 to 200 bars) values. In addition, several "realizations" with random combinations of symmetrical and asymmetrical circular cracks are considered.

The high-frequency (0.5Hz < f < 8.0Hz) ground motions are simulated using the stochastic modeling approach (see e.g., Boore, 1983; Shinozuka, 1988) by assuming that each circular crack of Figure 4 has been replaced by a double-couple point dislocation source whose position coincides with the center of the crack. Thirty ground motion realizations are computed for each scenario. The soil category considered in our study is NEHRP site class D consistent with the prevailing soil condition in the western part of the Anchorage basin (Dutta et al., 2000). The three independently derived ground motion components are then properly combined to generate synthetic broadband ground motion time histories and response spectra for the city of Anchorage due to the 1964 Prince William Sound earthquake.

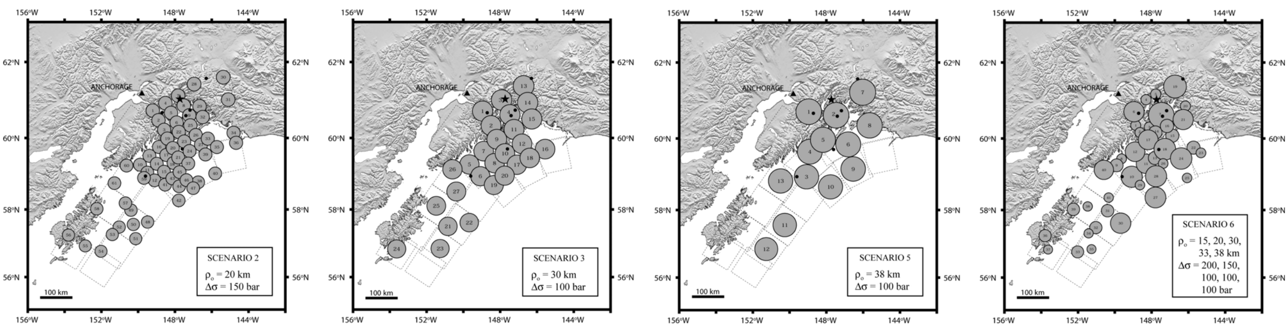

Figure 4. Scenarios considered for the intermediate-frequency strong ground motion simulations.

3.2. Simulation Results

After compiling the suite of time histories generated by the intermediate and high-frequency ground motion simulations described above, the 5% damped elastic response spectra of Figure 5 are obtained for the city of Anchorage. The gray area represents the range of response defined by the output of our realizations. The two black solid lines denote the mean-plus-one-standard-deviation response spectra in the intermediate and high-frequency ranges assuming a lognormal distribution of the response spectral values. The two gray solid lines indicate the response spectra in the intermediate-frequency range corresponding to the special cases of exclusively symmetrical (thin line) or asymmetrical (thick line) circular cracks. Finally, the dashed lines indicate the empirical response spectra for M=9.2 obtained based on the strong ground motion attenuation relationships proposed by Crouse (1991) and Youngs et al. (1997) for subduction zone earthquakes.

There is remarkable continuity in the response spectra of the NS and vertical ground motion components considering that a combination of deterministic and stochastic ground motion simulation techniques was exploited to simulate the response at the city of Anchorage. On the other hand, there is a discontinuity in the response spectra of the EW ground motion component at the interface of the intermediate and high-frequency ranges (f = 0.5Hz) attributed to the fact that the stochastic modeling approach cannot consider directivity effects and thus distinguish between intensities of horizontal ground motion components. Therefore, it is possible that our high-frequency simulation results overestimate the intensity of the high-frequency ground motions in the EW direction.

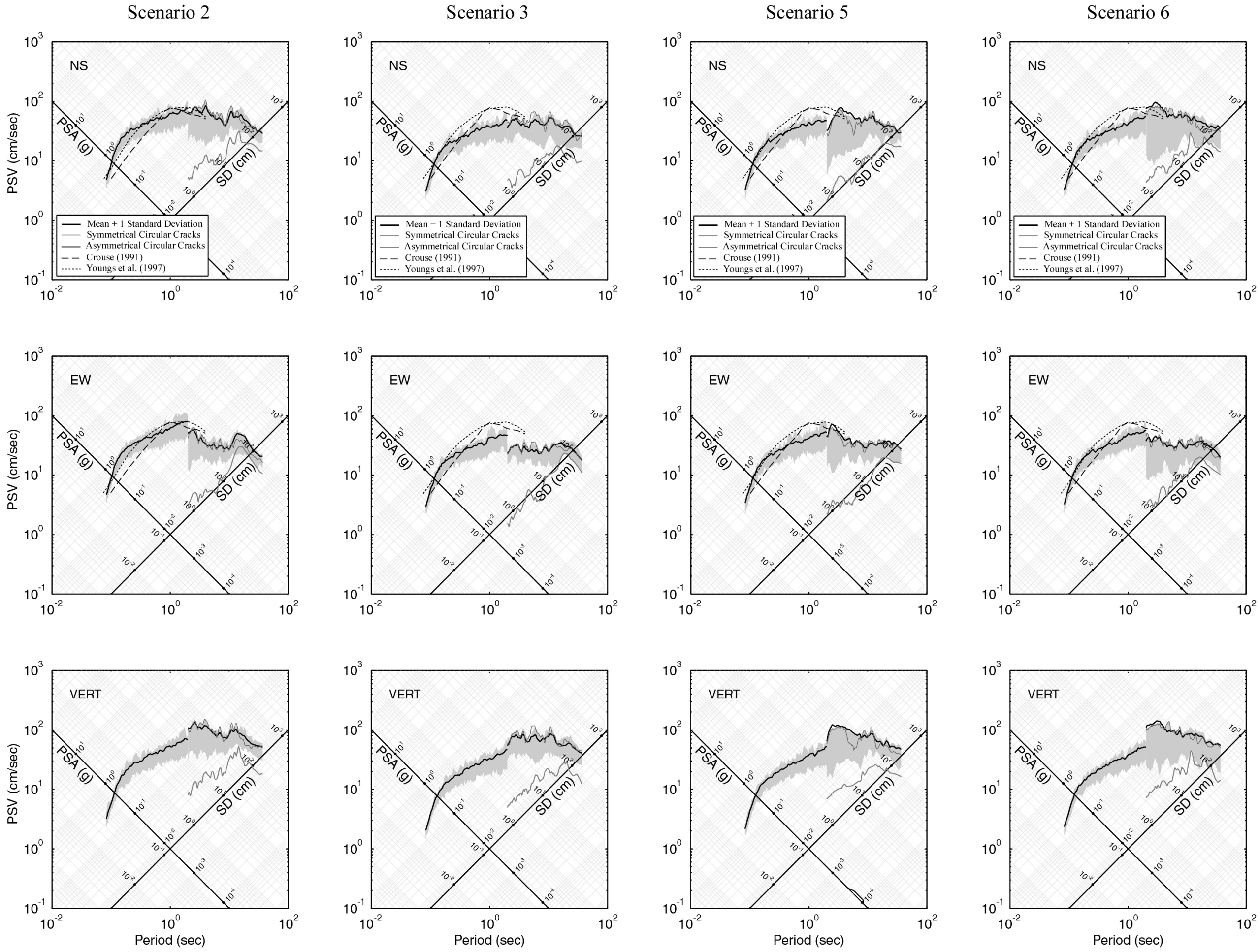

Figure 5. Synthetic elastic response spectra (5% damping) at the city of Anchorage obtained by compiling the intermediate- and high-frequency ground motion simulation results.

The response spectra of Scenario 2 are in good agreement with the empirical response spectra obtained using the ground motion attenuation relationships of Crouse (1991) and Youngs et al. (1997) as indicated in Figure 5. On the other hand, Scenarios 3, 5 and 6 yield response spectra with amplitudes smaller than those predicted by the attenuation equations; however, the mean synthetic spectra are lying within the range defined by the standard deviation of the ground motion attenuation relationships. This observation indicates that a smooth-type uniform rupture consisting of a large number of small circular cracks produces response spectra that are close to the average response spectra expressed by the ground motion attenuation relationships.

It should be emphasized that the gray area of Figure 5 represents the range of response defined by the outcome of our realizations; it does not intend to represent the entire uncertainty that characterizes the problem under investigation. In general, there are many factors that contribute to the total uncertainty of the strong motion numerical predictions. In our simulations, we have considered several scenarios and a large number of realizations. However, there are infinite rupture modes that one may consider pertaining to the properties of the circular cracks and their location on the subfault planes. Therefore, the synthetic time histories and response spectra presented in this study should be seen as plausible, but not necessarily unique, ground motions that capture the gross features of the 1964 Alaska earthquake.

Figure 6 displays typical acceleration, velocity and displacement time histories, as well as their corresponding elastic response spectra for Scenario 2; they were obtained by combining low-, intermediate- and high-frequency ground motion simulation results for the city of Anchorage using matched filtering at the crossover frequencies. We have selected to present time series from Scenarios 2 since this scenario yields results similar to the predictions of the ground motion attenuation relationships. The peak horizontal ground acceleration that the city of Anchorage sustained in the 1964 Alaska earthquake was of the order of 0.30g, while the duration of the seismic excitation was approximately 250s. It should be pointed out that the acceleration time histories are characterized by three distinct time intervals of high ground motion intensity. This feature is identified in the majority of the acceleration time series generated by our simulations.

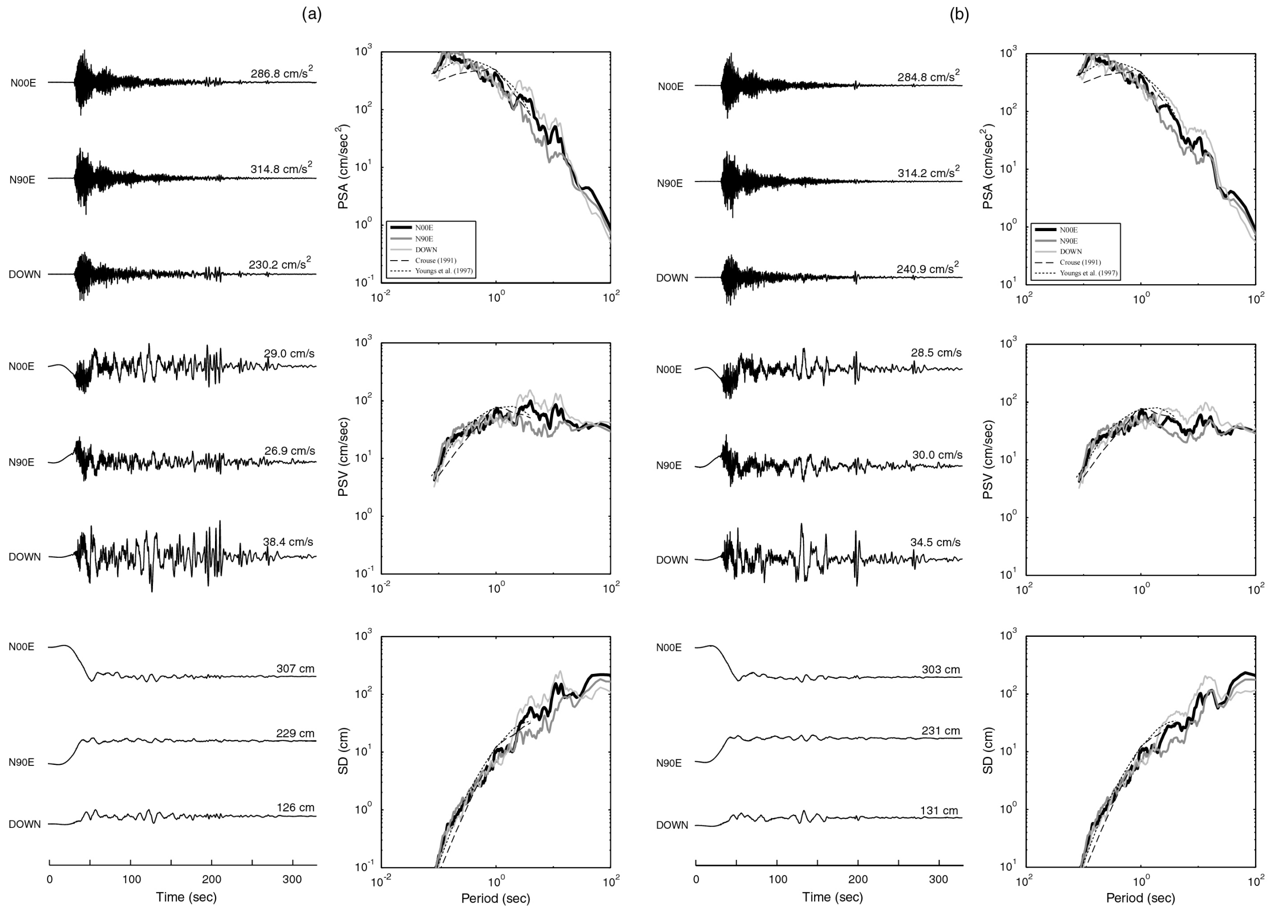

Figure 6. Characteristic broadband ground motion time histories (acceleration, velocity, displacement) and elastic response spectra (5% damping) at the city of Anchorage obtained by combing low-, intermediate- and high-frequency ground motion simulation results.

4. VALIDATION OF GROUND MOTION SIMULATION RESULTS

The low-frequency ground motion simulation results that dominate the permanent displacement field are in good agreement with the distribution of tectonic deformation induced by the 1964 Alaska earthquake (Plafker, 1965 and 1969; Parkin, 1967; Snay et al., 1987). It should be pointed out that the accuracy of the long-period ground motion simulations reflects, to a great extent, on the precision of the slip inversion itself since geodetic data were exploited for the derivation of the fault slip model proposed by Johnson et al. (1996).

The most important information regarding the variation of intensity of ground motion at Anchorage was recovered on a tape recorder that happened to be in use during the earthquake (Hudson and Cloud, 1973; Housner and Jennings, 1973). The noise of furniture rattling, house creaking together with the owner's comments permitted the time history of the intensity of shaking to be sketched. The shaping function of the amplitude of ground acceleration inferred by Housner and Jennings (1973) and typical synthetic acceleration time histories are illustrated in Figure 7. The agreement is excellent in terms of variation of ground motion intensity and total duration of seismic excitation. According to Seed and Wilson (1967), the duration of the ground shaking was also timed by means of watches by at least six people in and outside the Anchorage area. The observed durations ranged from 4.5 to 7.5 minutes. Seed and Wilson (1967) attributed the large landslide along the coastline in the Turnagain Heights area in Anchorage to the loss of strength in the underlying soils caused by the large duration of the ground shaking.

Hanson (1973) described the characteristics of an unanchored turbine fuel storage tank in Anchorage that failed (i.e., damage to roof and top wall, shell buckling at the bottom) in the 1964 Prince William Sound earthquake. We are exploiting the parameters and the simplified methodology regarding the response of tanks to earthquakes adopted by Hanson (1973) in an attempt to validate the spectral acceleration amplitudes of the synthetic ground motions. We are aware that other more accurate modeling approaches exist in the literature pertaining to the response of unanchored storage tanks to seismic excitations. However, we adopt the approach presented by Hanson (1973) since basic parameters of the tank are unknown (e.g., wall thickness, bottom-plate thickness, Young's modulus) and only a rough estimate of the spectral acceleration is needed. By assuming that the peak ground acceleration was in the range of 0.25g to 0.30g (see Figure 6), we conclude that the lightly damped spectral velocity at 3.9s should have been at least 25 to 30cm/s to generate the compressive force that according to Hanson (1973) was sufficient to account for the observed damage (i.e., buckling of tank's shell). This value can be considered as a lower bound of the spectral acceleration at 3.9s that is indeed in good agreement with the response spectra of Figure 6 (even though their damping ratio is 5%).

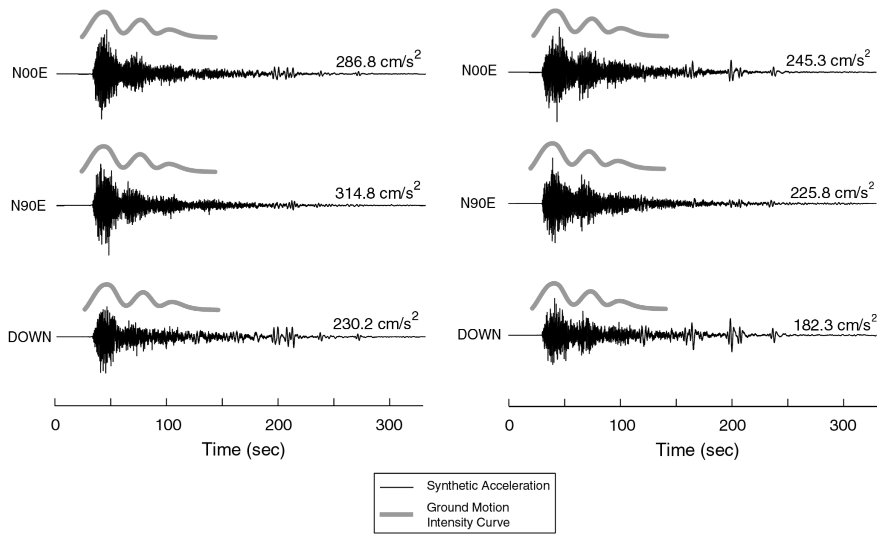

Figure 7. Comparison of the variation of intensity of the synthetic acceleration time histories at Anchorage with the ground motion shape function inferred by Housner and Jennings (1973).

5. SUMMARY

We have generated long-period strong ground motions on a dense grid of points extending over the shallow dipping fault of the 1964 Prince William Sound earthquake, as well as synthetic broadband ground motion time histories and response spectra for the city of Anchorage. The synthetic near-field ground motions are compatible with available seismological data, tectonic information, and eyewitness accounts pertaining to the 1964 Alaska earthquake. However, it should be pointed out that the simulated ground motions, while physically plausible, are not necessarily unique, nor incorporate the total uncertainty that characterizes the problem under investigation. Given that no strong motion records of giant earthquakes are presently available, the generated ground motion time histories and response spectra can be used to assess the performance of structures to large earthquakes.

ACKNOWLEDGEMENTS

This work was supported in part by the Earthquake Engineering Research Centers Program of the National Science Foundation under Award Number EEC-9701471 to the Multidisciplinary Center for Earthquake Engineering Research (Contract Numbers MCEER 99-0102 and 00-0102) and by the Alaska Science and Technology Foundation Grant Numbers 91-2-125 and 97-3-1312.

REFERENCES

Aki, K. (1983). Strong motion seismology, in *Earthquakes: Observation, Theory and Interpretation*, H. Kanamori and E. Boschi (Editors), *Proc. Int. Sch. Phys. Enrico Fermi*, Course LXXXV, 223-250, North-Holland Publ., Amsterdam.

Boore, D. M. (1983). Stochastic simulation of high-frequency ground motions based on seismological models of the radiated spectra, *Bull. Seism. Soc. Am.* **73**, 1865-1894.

Bouchon, M. (1979). Discrete wave number representation of elastic wave fields in three-space dimensions, *J. Geophys. Res.* **84**, 3609-3614.

Bouchon, M., and K. Aki (1977). Discrete wave-number representation of seismic-source wave fields, *Bull. Seism. Soc. Am.* **67**, 259-277.

Brune, J. N. (1970). Tectonic stress and the spectra of seismic shear waves from earthquakes, *J. Geophys. Res.* **75**, 4997-5009.

Christensen, D. H., and S. L. Beck (1994). The rupture process and tectonic implications of the Great 1964 Prince William Sound earthquake, *Pure Appl. Geophys.* **142**, 29-53.

Crouse, C. B. (1991). Ground-motion attenuation equations for earthquakes on the Cascadia subduction zone, *Earthquake Spectra* **7**, 201-236.

Dong, G., and A. S. Papageorgiou (2002). Seismic radiation from a unidirectional asymmetrical circular crack model, Part I: Constant rupture velocity, *Bull. Seism. Soc. Am.* **92**, 945-961.

Dutta, U., N. Biswas, A. Martirosyan, S. Nath, M. Dravinski, A. Papageorgiou, and R. Combellick (2000). Delineation of spatial variation of shear wave velocity with high-frequency Rayleigh waves in Anchorage, Alaska, *Geophys. J. Int.* **143**, 365-375.

Furumoto, A. S. (1965). Analysis of Rayleigh wave. Part II in Source Mechanism Study of the Alaska Earthquake and Tsunami of March 27, 1964, *Report HIG-65-17*, University of Hawaii, Institute of Geophysics, Honolulu, Hawaii, 31-42.

Hanson, R. D. (1973). Behavior of liquid-storage tanks, in *The Great Alaska earthquake of 1964: Engineering*, National Academy of Science, Washington D.C., 331-339.

Housner, G. W., and P. C. Jennings (1973). Reconstituted earthquake ground motion at Anchorage, in *The Great Alaska earthquake of 1964: Engineering*, National Academy of Science, Washington D.C., 43-48.

Hudson, D. E., and W. K. Cloud (1973). Seismological background for engineering studies of the earthquake, in *The Great Alaska earthquake of 1964: Engineering*, National Academy of Science, Washington D.C., 18-42.

Johnson, J. M., K. Satake, S. R. Holdahl, J. Sauber (1996). The 1964 Prince William Sound earthquake: Joint inversion of tsunami and geodetic data, *J. Geophys. Res.* **101**, 523-532.

Kanamori, H. (1970). The Alaska earthquake of 1964: Radiation of long-period surface waves and source mechanism, *J. Geophys. Res.* **75**, 5029-5040.

Luco, J. E, and R. J. Apsel (1983). On the Green's functions for a layered half-space, Part I, *Bull. Seism. Soc. Am.* **73**, 909-929.

Mavroeidis, G. P., B. Zhang, G. Dong, A. S. Papageorgiou, U. Dutta, and N. N. Biswas (2008). Estimation of strong ground motion from the Great 1964 Prince William Sound, Alaska, earthquake (M_w=9.2), *Bull. Seism. Soc. Am.* (in press).

Parkin, E. J. (1967). Horizontal crustal movements determined from surveys after the Alaskan earthquake of 1964, in *The Prince William Sound, Alaska, earthquake of 1964 and aftershocks, Volume III: Geodesy and Photogrammetry*, U.S. Department of Commerce, Washington D.C., 35-50.

Plafker, G. (1965). Tectonic deformation associated with the 1964 Alaskan earthquake, *Science* **148**, 1675-1687.

Plafker, G. (1969). Tectonics of the March 27, 1964, Alaska earthquake, *U.S. Geological Survey Professional Paper 543-I*, 1-74.

Sato, T., and T. Hirasawa (1973). Body wave spectra from propagating shear cracks, *J. Phys. Earth* **21**, 415-431.

Seed, H. B., and S. D. Wilson (1967). The Turnagain Heights landslide, Anchorage, Alaska, *J. Soil Mech. Found. Div. ASCE* **93**, 325-353.

Sherburne, R. W., S. T. Algermissen, and S. T. Harding (1969). The hypocenter, origin time, and magnitude of the Prince William Sound earthquake of March 28, 1964 in *The Prince William Sound, Alaska, Earthquake of 1964 and Aftershocks*, U.S. Department of Commerce, Washington, D.C., 49-69.

Shinozuka M (1988). State-of-the-art report: Engineering modeling of ground motion. *Proceedings of the 9th World Conference on Earthquake Engineering,* Tokyo, Japan, August 2-9.

Snay, R. A., M. W. Cline, and E. L. Timmerman (1987). Project REDEAM: Models for historical horizontal deformation, *NOAA Technical Report NOS 125 NGS 42*.

Wyss, M., and J. N. Brune (1967). The Alaska earthquake of 28 March 1964: A complex multiple rupture, *Bull. Seism. Soc. Am.* **57**, 1017-1023.

Youngs, R. R., S.-J. Chiou, W. J. Silva and J. R. Humphrey (1997). Strong ground motion attenuation relationships for subduction zone earthquakes, *Seism. Res. Lett.* **68**, 58-73.